

Supporting information

C-14 powered dye-sensitized betavoltaic cells

Yunju Hwang,^{a,‡} Young Ho Park,^{a,‡} Hong Soo Kim,^{a,‡} Dae Hee Kim,^a Shahzad Ali,^a Saurav Sorcar,^a Monica Claire Flores,^a Michael R. Hoffmann,^b Su-Il In^{a,b*}

^aDepartment of Energy Science & Engineering, Daegu Gyeongbuk Institute of Science & Technology (DGIST), 333 Techno Jungang-daero, Hyeonpung-eup, Dalseong-Gun, Daegu, 42988, Republic of Korea

^bLinde + Robinson Laboratories, California Institute of Technology, Pasadena, California 91125, United States of America

*Correspondence to: S.-I. In (e-mail: insuil@dgist.ac.kr)

‡ These authors contributed equally to this work

Experimental

Chemicals

For the fabrication of TiO₂ electrode, TiO₂ paste (18 NR-T, Dyesol, Australia, Average nanoparticle size 20 nm) was purchased from Hanalintech Inc., Republic of Korea. Furthermore for the dye, *cis*-bis(isothiocyanato)-bis(2,2'-bipyridyl 4,4' dicarboxylato) ruthenium(II)bis-tetrabutylammonium (D719, Everlight Chemical Industrial Crop., Taiwan, commonly called N719 dye), *cis*-diisothiocyanato-bis(2,2'-bipyridyl-4,4'-dicarboxylic acid) ruthenium(II) (Ruthenizer 535, Solaronix SA, Switzerland, commonly called N3 dye), and 5-carboxy-2-[[3-[(2,3-dihydro-1,1-dimethyl-3-ethyl-1H-benzo[e]indol-2-ylidene)methyl]-2-hydroxy-4-oxo-2-cyclobuten-1-ylidene]methyl]-3,3-dimethyl-1-octyl-3H-indolium (Sensidizer SQ2, Solaronix SA, Switzerland). Also, ¹²C-citric acid (ACS reagent, ≥ 99.5%, Sigma aldrich), ammonium hydroxide (ACS, 28.0 ~ 30.0%, Alfa Aesar) and ethyl alcohol (Anhydrous, 99.9%, Daejung Chemicals & Metals Co., LTD, Republic of Korea) were used. For the electrolyte, I⁻/I₃⁻ organic solvent-based electrolyte solution (EL-HPE, Dyesol, Australia) was used. ¹⁴C-citric acid was from American radiolabeled chemicals (ARC, USA).

Preparation of Novel Nano/Quantum Carbon Dots Electrode Betavoltaic Cell

The fabrication method of TiO₂ electrode was adopted from the previously published paper.¹⁻⁷ To fabricate TiO₂ electrode, fluorine-doped tin oxide (FTO) coated glass plates (TEC7, Pilkington, United States of America) were purchased from Hanalintech Inc., Republic of Korea, with dimension of 25 mm × 10 mm and 2.2 mm thickness. The FTO glass was ultrasonically cleaned with anhydrous ethyl alcohol (99.9%) for 30 min and dried using nitrogen gas. After that, 22 mm × 4 mm frame was assembled in the center of FTO glass and edges were covered with the 3M magic tapes. The remaining FTO glass frame was coated with TiO₂ paste

by doctor blade technique using a thin glass rod. After that, the 3M magic tapes were removed and the electrode was dried at 70 °C for 30 min followed by sintering at 450 °C, 5 °C min⁻¹ for 30 min in box furnace. The furnace was allowed to cool down naturally up to 80 °C. After cooling, the electrode was immersed in 0.5 mM solution of dye (N719, N3 and SQ2) containing anhydrous ethyl alcohol, in order to make a dye-sensitized TiO₂ electrode, at room temperature for 24 h. After the dye immersion, the electrode was washed with anhydrous ethanol, and dried using nitrogen gas. Finally, the dye-coated TiO₂ electrode was removed by trimming to leave only the working area of 10 mm × 4 mm and then the impurities were blown out by the nitrogen gas.

To assemble the nano/quantum carbon particle electrode betavoltaic cell, 60 μm thick Surlyn (Meltonix 1170-60, Solaronix, Switzerland) was placed in between the TiO₂ electrode and carbon electrode (carbon-12 or carbon-14), and heated to 120 °C for sealing. After sealing, the distance is the ≈ 43 μm (TiO₂ thickness ≈ 7 μm and Surlyn thickness 50 μm, in the Fig. S1) between carbon electrode and TiO₂ electrode. Afterward, a micropipette was used to poke a hole on the carbon electrode wherein the electrolyte solution was injected to prevent bubble formation and to remove any residues from the electrode. Then, the holes on the carbon counter electrode were covered with Surlyn and glass pieces; and then finalized with heating.

Preparation of Carbon Electrode

The N-carbon (nitrogen doped carbon) dots were synthesized by a direct pyrolysis method reported by Wang *et al.*⁸ To make carbon counter electrode, washed FTO glass with hole and precursor solution was prepared. Mixed solution was made up of 4 mg citric acid, 9 mL deionized water and 1 mL ethanol. The mixed solution has the same concentration as the purchased radioisotope citric acid (carbon-14). After that, 1 mL ammonia solution was mixed

with 10 mL mixed solution. Then 0.6 μL of precursor solution was poured dropwise on the FTO glass with drying at 80 $^{\circ}\text{C}$. After drying, the sample was calcinated in a box furnace at 200 $^{\circ}\text{C}$ for 3 h, at a rate of 10 $^{\circ}\text{C min}^{-1}$. Drop and calcination processes were repeated five times.

Characterization of TiO_2 and Carbon Electrode

A TiO_2 electrode on the FTO glass was analysed by field emission scanning electron microscope (FE-SEM) (**Fig. S1**). **Fig. S1(A)** shows the top-view of the electrode with TiO_2 particles (purple region) covering the FTO layer (yellow region). TiO_2 particles are highly dense with an average size of 20 nm. The TiO_2 paste thickness is 6.23 μm as shown in **Fig. S1(B)**.

Due to safety regulations (**Table S1**), both chemical and morphological studies were conducted using a C-12 counter electrode instead of C-14 deriving from the concept of isotopes possessing similar chemical properties but different atomic weights.⁹ **Fig. S2(A)** and **(B)** show FE-SEM images of bare FTO glass and FTO glass uniformly coated with carbon nanoparticles and quantum dots. **Fig. S2(C)** transmission electron microscope (TEM) confirms the presence of carbon quantum dots, with a diameter of ≈ 5.76 nm; the d-spacing of 0.21 nm, **Fig. S2(D)**, obtained from high-resolution transmission electron microscope (HR-TEM) corresponds to the (100) plane of graphene.^{10,11} In order to increase the density of beta rays, sub-nano meter carbon quantum dots were utilized whose size is confirmed by SEM and TEM.

The nano/quantum carbon dot mixture imparts both high surface area and porosity, thereby facilitating faster electron transport. X-ray diffractions (XRD) spectra of the carbon dots show 2 θ peaks at 24.69 $^{\circ}$ and 42.67 $^{\circ}$ which correspond to the (002) and (100) in-planes for hexagonal graphite (**Fig. S3(A)**).¹²⁻¹⁴ Raman spectroscopy, see **Fig. S3(B)**, reveal two peaks at 1357 cm^{-1}

and 1568 cm^{-1} , which corresponds to the sp^3 defects (D-band) and sp^2 carbon (G-band) in the carbon nano/quantum dots, respectively.¹⁴

X-ray photoelectron spectroscopy (XPS) analysis confirms the presence of nitrogen doping and a variety of polar groups in the nano/quantum carbon dots. The survey spectrum (**Fig. S4(A)**) reveals the existence of carbon (C 1s, 284.5 eV), nitrogen (N 1s, 399.8 eV), and oxygen (O 1s, 531.8 eV). The main peaks of C 1s appeared at 284.5 eV, 286.2 eV, and 288.3 eV (**Fig. S4(B)**). Based on the energy of 284.5 eV the binding energy of the C-C bonds, a correction value was given for all binding energies.¹⁵⁻¹⁸ Binding energy peaks at 286.2 eV, and 288.3 eV in the C 1s spectrum are attributed to C-N, C-O, and C=O bonds, respectively.¹⁹ Nitrogen doping in the nano/quantum carbon dots electrode is established by deconvolution of **N 1s** XPS spectra, **Fig. S4(C)**. The binding energy positioned at 399.8 eV confirms C-N bond formation, which is primarily due to ammonia being used during the synthesis.⁸ **Fig. S4(D)** shows the O 1s peak. Upon deconvolution, peaks at 531.8 eV and 533.2 eV are attributed to C=O and C-O bonding, respectively.^{8, 20}

Equipment used

Surface morphologies were analyzed at 3 kV and 10 μA , using field emission scanning electron microscope (FE-SEM, Hitachi, SU 8020). Also, field emission transmission electron microscope (FE-TEM, Hitachi, HF-3300) was used to confirm the size and lattice spacing of the carbon quantum dots; the samples were fabricated by the above-mentioned experimental method and using the centrifuge to separate the carbon quantum dots particles. To obtain the pattern of nano/quantum carbon particles, X-ray diffraction (XRD, Rigaku, Miniflex 600) was used with a Panalytical, Empyrean X-ray diffractometer using Cu $K\lambda$ radiation ($\lambda = 1.54\text{ \AA}$). Raman spectra of the nano/quantum carbon were obtained with a Raman spectrometer (Thermo Scientific,

Nicolet Almeca XR) with a 532 nm laser used for excitation. The binding structure and properties of the samples were analyzed by X-ray photoelectron spectroscopy (XPS, Thermo Scientific, ESCALAB 250Xi) with the Al X-ray source (1486.6 eV). To confirm the performance and analyze the cells, sourcemeter (Keithley, 2635B) was used at -0.05 ~ 0.8 V condition.

Supplementary Text

Equation S1. Calculations for the efficiency of betavoltaic cell.

$$\eta = \frac{P_{max}}{P_{source}} \times 100\% = \frac{J_{sc} \times V_{oc} \times FF}{(3.7 \times 10^7) \times \emptyset \times E_{avg} \times e \times A} \times 100\% \quad (S1)$$

P_{max} : The maximum output power of the Betavoltaic device (W)

P_{source} : The radiation power of the ^{14}C source (W)

FF : Fill factor (Taken from Table. S2)

V_{oc} : Open circuit voltage (V) (Taken from Table. S2)

I_{sc} : Short circuit current (A) (Taken from Table. S2)

\emptyset : The source activity (Ci) = 0.02727 mCi for C-14

Active Area: 0.4 cm²

1 Ci = 3.7×10^{10} Bq = 3.7×10^{10} Decay/s

E_{avg} : The average beta energy of the isotope (eV/Decay) = 49.4 keV/Decay for C-14

e : Electron charge (C)

Putting values in equation (1)

$$= \frac{12.75 \text{ nA/cm}^2 \times 29.2 \text{ mV} \times 0.255}{(3.7 \times 10^7 \text{ Bq/mCi})(1 \text{ Decay/Bq} \cdot \text{s})(0.02727 \text{ mCi})(49.4 \text{ keV/Decay})} \times 100\%$$

$$= \frac{5.10 \text{ nA} \times \{1e/(1.6 \times 10^{-19} \text{ C})\} \times \{(1.6 \times 10^{-19} \text{ C}/1e)\} \times 29.2 \text{ mV} \times 0.255}{(1.0090 \times 10^6 \text{ Decay/s}) \times (7.904 \times 10^{-15} \text{ J/Decay})} \times 100\%$$

$$= \frac{(3.1875 \times 10^{10} \text{ electron/s}) \times (11.914 \times 10^{-22} \text{ J/electron})}{(1.0090 \times 10^6 \text{ electron/s}) \times (7.904 \times 10^{-15} \text{ J/electron})} \times 100\%$$

$$= \frac{0.038 \text{ nW}}{7.975 \text{ nW}} \times 100\% = 0.48\%$$

FF in our case is less than 25 which may be attributed to low carbon concentration of counter electrode²¹

Equation S2. Calculations for the Enhancement of electrons.

$$\frac{\text{Number of electrons from DSBC per second}}{\text{Number of electrons emitted from source per second}} = \frac{I_{sc}}{(3.7 \times 10^7) \times \phi} \quad (2)$$

I_{sc} : Short circuit current (A)

ϕ : The source activity (Ci)

$$1 \text{ Ci} = 3.7 \times 10^{10} \text{ Bq} = 3.7 \times 10^{10} \text{ Decay/s}$$

Putting values in equation (2)

$$\begin{aligned} &= \frac{5.10 \text{ nA}}{(3.7 \times 10^7 \text{ Bq/mCi})(1 \text{ Decay/Bq} \cdot \text{s})(0.02727 \text{ mCi})} \\ &= \frac{5.10 \text{ nA} \times \{1e/(1.6 \times 10^{-19} \text{ C})\}}{(3.7 \times 10^7 \text{ Bq/mCi})(1 \text{ Decay/Bq} \cdot \text{s})(0.02727 \text{ mCi})(1 \text{ electron/Decay})} \\ &= \frac{3.1875 \times 10^{10} \text{ electron/s}}{1.0090 \times 10^6 \text{ electron/s}} = 3 \times 10^4 \end{aligned}$$

Equation S3. Calculations for energy generated from radioactive isotope(C-14)

$$P(0)W/Ci = \text{Average energy(keV/Decay)} \times 3.7 \times 10^{10} (\text{Decay/s}\cdot\text{Ci}) \times 1000 (\text{eV/keV}) \times 1.6 \\ \times 10^{-19} (\text{J/eV}) = 292.448 \text{ uW/Ci}$$

P(0)W/Ci: The power emitted by the isotope at the beginning of its into the device

¹⁴Carbon Average energy: 49.4 keV

Energy generated from radioactive isotopes: 7.97 nW (When used 0.02727mCi)

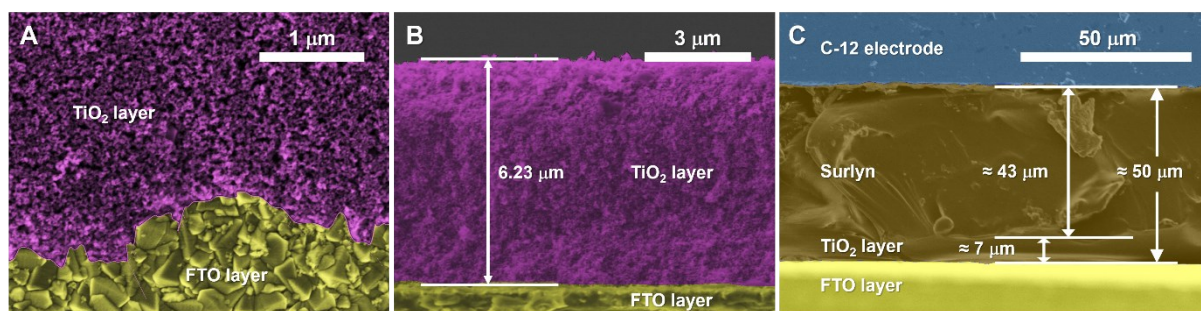


Fig. S1. FE-SEM images of (A) top-view and (B) cross-section side-view of TiO₂ electrode and (C) side-view of C-12 electrode cell.

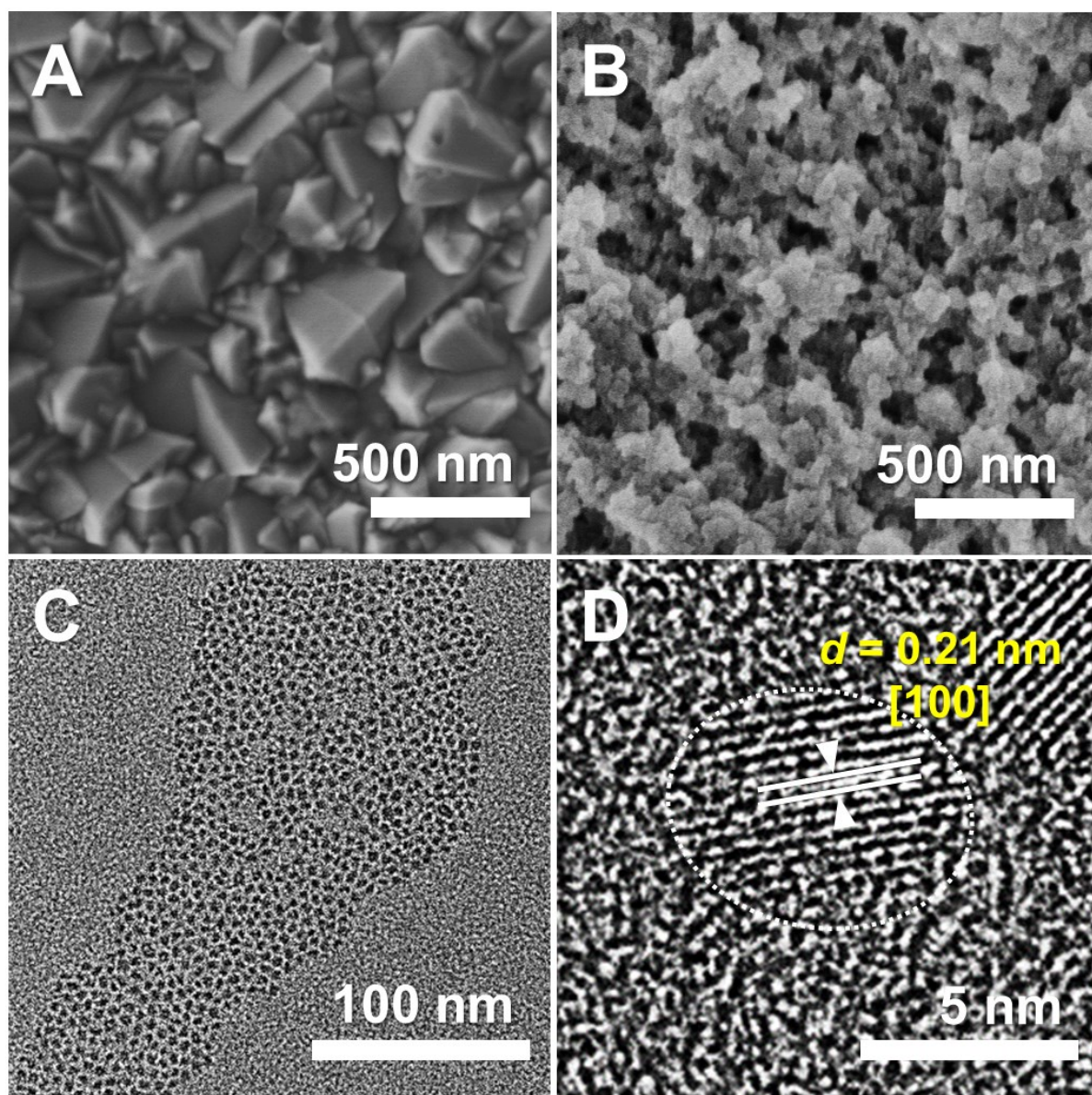


Fig. S2. FE-SEM images of: (A) the bare FTO glass and (B) nano/quantum carbon dots on the FTO glass. (C) FE-TEM and (D) high-resolution TEM images of the carbon quantum dots.

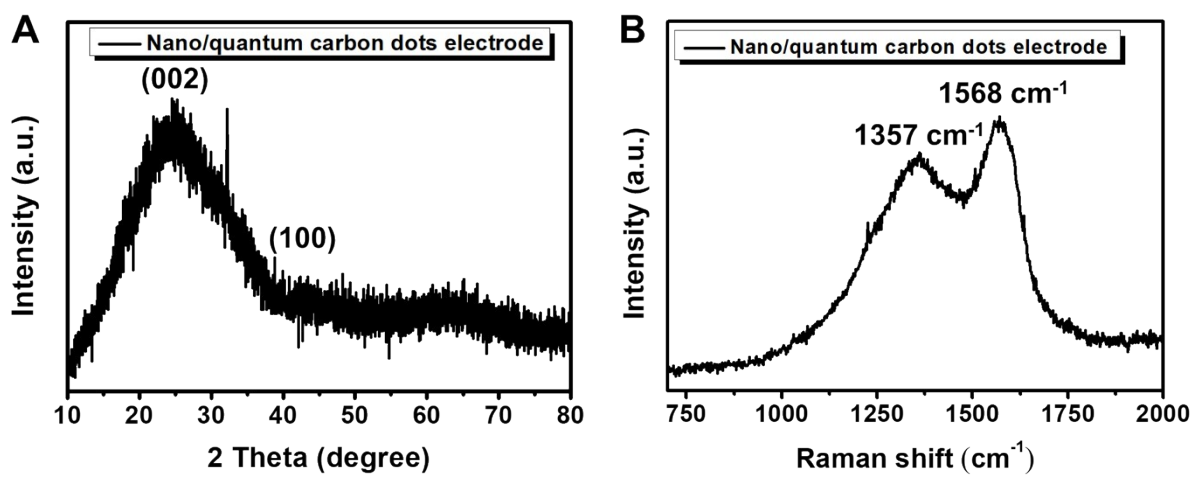


Fig. S3. (A) XRD and (B) Raman analysis of nano/quantum carbon dots electrode.

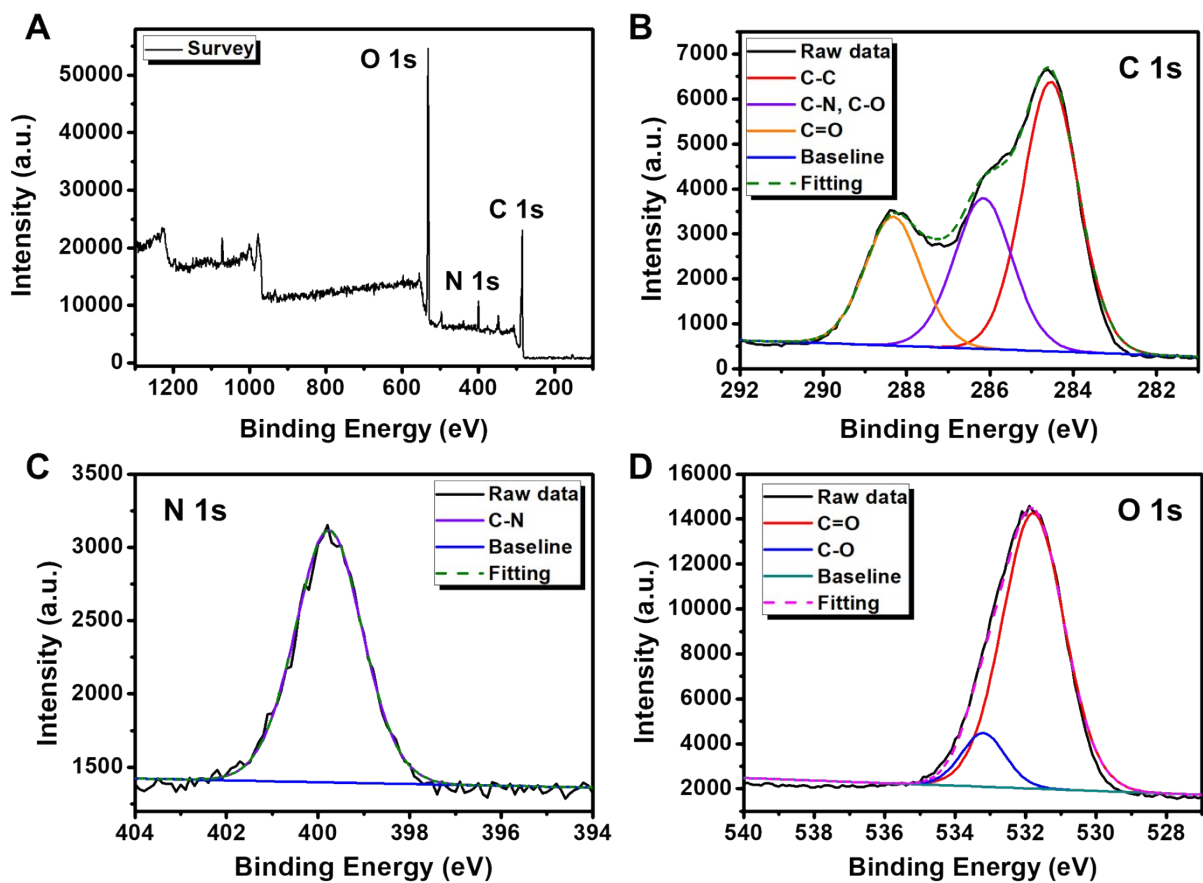


Fig. S4. XPS analysis of nano/quantum carbon dots on the FTO glass: (A) survey, (B) C 1s, (C) N 1s, and (D) O 1s.

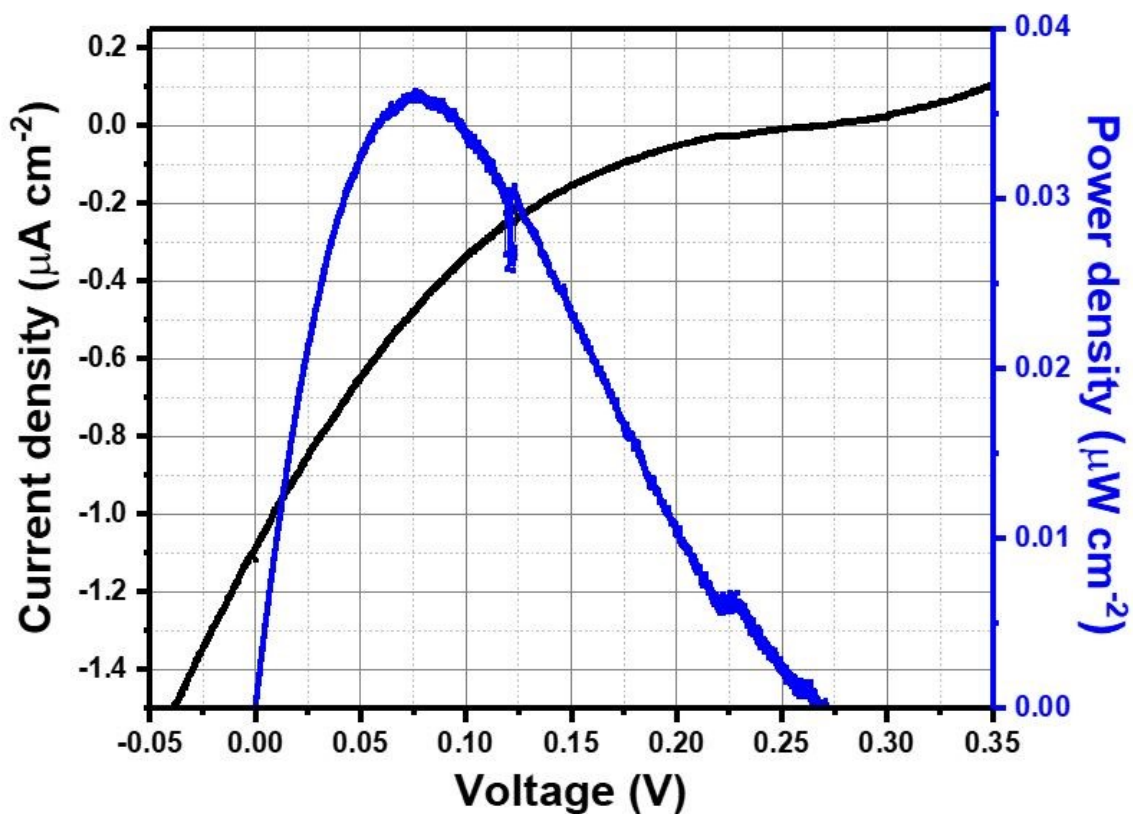


Fig. S5. J-V/P-V performance of the pristine cell (No dye/Radiation) under UV irradiation test.

Explanation: The betavoltaic battery without dye under **6 W** UV irradiation generated more short-circuit current ($2.788 \mu\text{A}$) and open circuit voltage (0.268 V) with a power density of $0.036 \mu\text{W cm}^{-2}$. This improved performance can be interlinked to higher amount of input energy supplied by UV-irradiations as compared to low energy (7.97 nW) of beta radiations, incapable to excite TiO_2 .

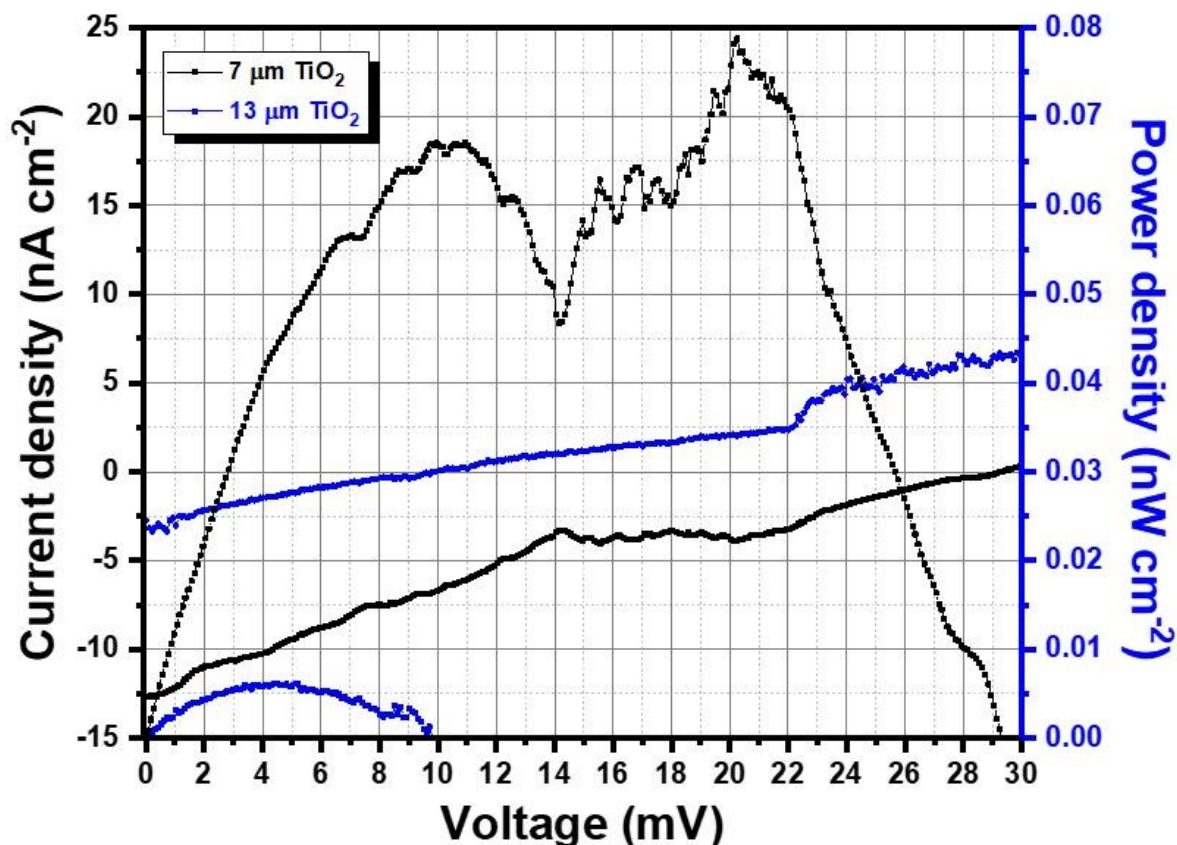


Fig. S6. J-V/P-V performance comparisons with different thickness of TiO₂.

Explanation: Thickness of the electrode is also prime factor which influences the performance of DSSC. To prepare samples of various thicknesses, the 3M tape layers are superimposed. Following this, the 7 μm thick electrode, equaling to minimum thickness of tape, single layer, was prepared. However, this method worked only for 2 layers to produce a thickness of 13 μm and beyond this, electrode was cracked when it was annealed. We tested this sample and results are shown in this figure, but the efficiency is low for increased thickness.

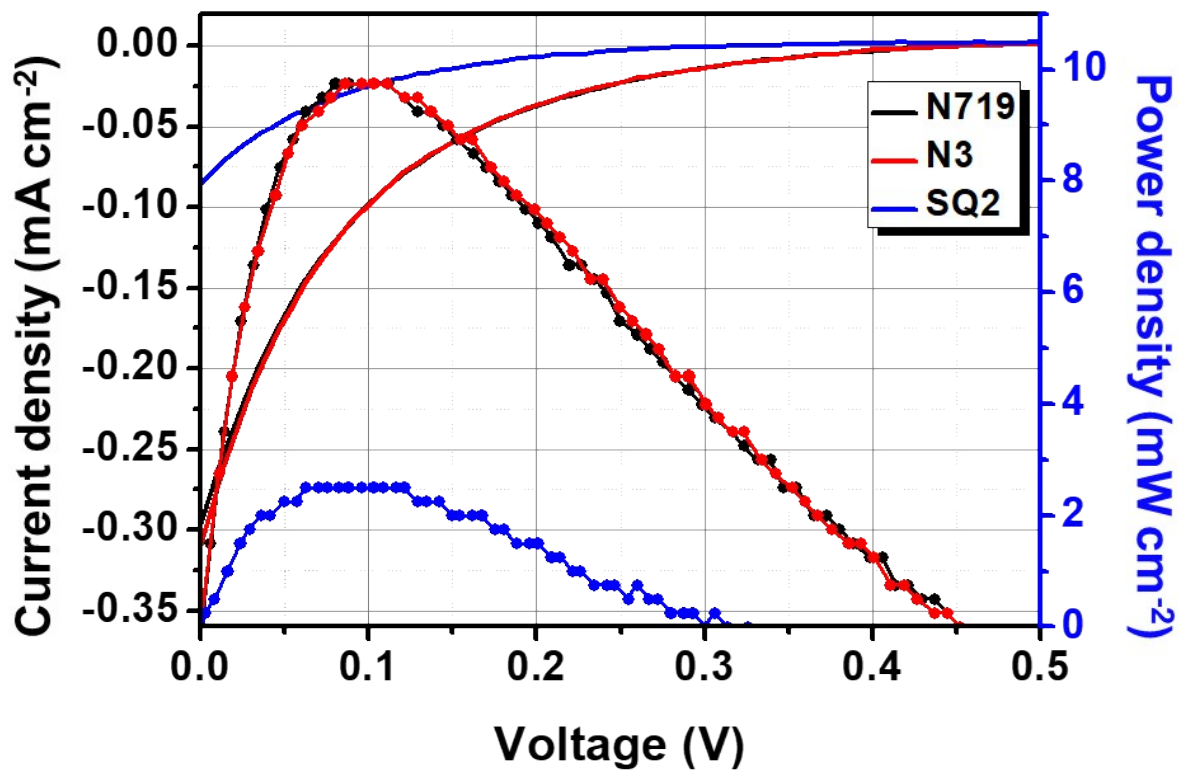


Fig. S7. J-V/P-V performance of ¹²C-DSSC under AM 1.5 by using solar simulator.

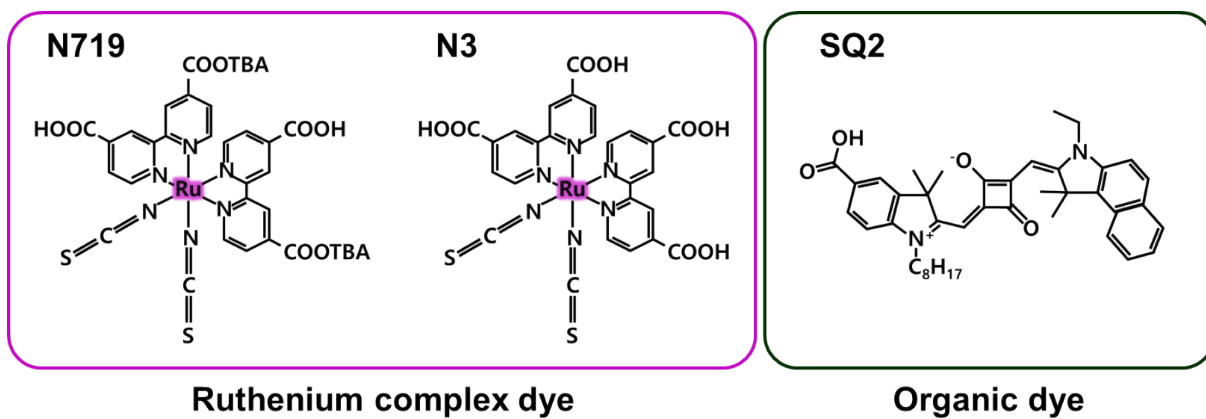


Fig. S8. The chemical structure of ruthenium complex dye (N719 and N3) and organic dye (SQ2).

Table S1. Safety regulations of nuclear materials handling.

	Article												
NUCLEAR SAFETY ACT²²	<p>Article 2 (Definitions) The terms used in this Act shall be defined as follows:<Amended by Act No. 11715, Mar.23, 2013; Act No. 12666, May 21, 2014; Act No. 13078, Jan. 20, 2015; Act No. 13389, Jun. 22, 2015; Act No. 13616, Dec. 22, 2015></p> <p>3. The term "nuclear fuel materials" means materials prescribed by Presidential Decree that produce nuclear energy, such as uranium and thorium;</p> <p>4. The term "nuclear raw materials" means uranium ore, thorium ore, and other materials prescribed by Presidential Decree, used as raw materials for nuclear fuel materials;</p> <p>6. The term "radioactive isotope" means an isotope which emits radiation and what is prescribed by Presidential Decree among any combination thereof;</p>												
ENFORCEMENT DECREE OF THE NUCLEAR SAFETY ACT²³	<p>Article 5 (Radioisotopes) "Isotope prescribed by Presidential Decree" in subparagraph 6 of Article 2 of the Act means any substance for which the quantity and concentration of an isotope exceed such quantity and concentration as determined by the Commission, excluding the following substances:</p> <p>1. Nuclear fuel material referred to in subparagraph 3 of Article 2 of the Act;</p> <p>2. Nuclear source material referred to in subparagraph 4 of Article 2 of the Act;</p> <p>3. Radioactive material or apparatuses in which radioactive material is embedded, which poses no risk of radiation hazard as determined and publicly notified by the Commission.</p>												
STANDARD OF RADIATION PROTECTION²⁴	<p>Article 9 (Quantity and Concentration of Radioisotopes) "Quantity and concentration as prescribed by the Nuclear Safety and Security Commission" as provided for in Article 5²³ of the Decree shall be the quantity in column 3 and the concentration in column 4 for the relevant radionuclides in column 2 of Table 5.</p> <table border="1" style="width: 100%; border-collapse: collapse; text-align: center;"> <thead> <tr> <th colspan="4">Quantity and Specific Activity of Radioisotopes for Exemption [Table 5]</th> </tr> <tr> <th style="width: 25%;">Atomic number [Column 1]</th> <th style="width: 25%;">Isotopes [Column 2]</th> <th style="width: 25%;">Minimum Quantity, (Bq) [Column 3]</th> <th style="width: 25%;">Minimum Specific Activity (Bq/g) [Column 4]</th> </tr> </thead> <tbody> <tr> <td>6</td> <td>C-14</td> <td>1×10^7</td> <td>1×10^4</td> </tr> </tbody> </table>	Quantity and Specific Activity of Radioisotopes for Exemption [Table 5]				Atomic number [Column 1]	Isotopes [Column 2]	Minimum Quantity, (Bq) [Column 3]	Minimum Specific Activity (Bq/g) [Column 4]	6	C-14	1×10^7	1×10^4
Quantity and Specific Activity of Radioisotopes for Exemption [Table 5]													
Atomic number [Column 1]	Isotopes [Column 2]	Minimum Quantity, (Bq) [Column 3]	Minimum Specific Activity (Bq/g) [Column 4]										
6	C-14	1×10^7	1×10^4										
Regulations on Technical Standards for Radiation Safety Control, Etc.²⁵	<p>Article 37 (Use and Distribution) Technical standards as regards the use or distribution of unsealed sources shall be as follows:</p> <p>1. Unsealed sources shall be used or distributed at use facilities or work rooms.</p>												

Table S2. Comparison of efficiency achieved from dye-sensitized betavoltaic cell (DSBC) with respect to control cells namely blank cell, dye-sensitized cell, and betavoltaic cell (No dye / Radiation).

Cell type	Open-circuit voltage (V_{oc} , mV)	Short-circuit current (J_{sc} , nA cm ⁻²)	Max power density (nW cm ⁻²)	Fill factor (FF)	Efficiency (η , %)
No dye / No radiation (blank cell)	5.15	2.098	-	0.237	-
Dye / No radiation (DSSC under dark)	2.91	1.113	-	0.267	-
No dye / Radiation (betavoltaic cell)	3.34	2.85	0.000225	0.226	0.001
Dye / Radiation (DSBC)	29.2	12.75	0.095	0.255	0.48

Table S3. A comparison of previous works reporting betavoltaic batteries and properties.

Type of battery Parameters	Radioactive source	Open-circuit voltage (V_{oc} , mV)	Short-circuit current density (J_{sc} , nA cm ⁻²)	Efficiency (η , %)	Researcher (Published year)
PN Junction	⁶³ Ni, 10 mCi	350	157	3.17	Faezeh Rahmani, <i>et al.</i> (2016) ²⁶
Betavoltaic Battery	⁶³ Ni, 10 mCi	151	72.9	0.6	Andrey Krasnov, <i>et al.</i> (2016) ²⁷
	⁶³ Ni, 1 mCi	720	16.8	6	M. V. S. Chandranshekar <i>et al.</i> (2005) ²⁸
	¹⁴⁷ Pm, 897 mCi·mg ⁻¹	1,120	14,766	9.40	
Schottky Junction	⁶⁰ Co, 1100 mCi·mg ⁻¹	1,130	18,419	5.76	A. Waris, <i>et al.</i> (2016) ²⁹
Betavoltaic Battery	⁶³ Ni, 11.7 mCi·mg ⁻¹	260	10.76	0.50	
	⁶³ Ni, 20 mCi	1,040	117.5	3.79	Y. Ma, <i>et al.</i> (2018) ³⁰
	⁶³ Ni, 30 μCi·mm ⁻²	100	1.2	0.32	M. Lu, <i>et al.</i> (2011) ³¹
	⁶³ Ni, 10 mCi	260	86.6	1.18	Faezeh Rahmani, <i>et al.</i> (2016) ²⁶
Nano/Quantum					
¹⁴Carbon Particle Electrode	¹⁴ C, 0.027 mCi	29.2	12.75	0.48	Our research
Betavoltaic Battery					

Table S4. Performance of ¹²C-DSSC under AM 1.5 by using solar simulator.

Dye type	Open-circuit voltage (V_{oc} , V)	Short-circuit current (J_{sc} , mA cm ⁻²)	Max power density (mW cm ⁻²)	Fill factor (FF)	Efficiency (η , %)
N719	0.454	0.31	9.5	6.8	0.009
N3	0.454	0.2975	10.25	7.6	0.010
SQ2	0.310	0.2125	2.25	8.3	0.002

Explanation: In addition to other parameters the output energy is strongly interlinked to input energy supplied as it can be seen from Table S2 and S4 for beta radiations and solar simulated light respectively. Since the solar radiations possess higher amount of energy than beta radiations thus output voltage is higher when DSSC is tested under them.

Table S5. Comparison of efficiency achieved from dye-sensitized betavoltaic cell (DSBC) with different dye; N719, N3 and SQ2 (No dye / Radiation).

Cell type	Open-circuit voltage (V_{oc} , mV)	Short-circuit current (J_{sc} , nA cm ⁻²)	Max power density (nW cm ⁻²)	Fill factor (FF)	Efficiency (η , %)
N719 / No radiation	2.91	1.113	-	0.267	-
N719 / Radiation	29.2	12.75	0.095	0.255	0.48
N3 / No radiation	0.112	0.103	-	0.331	-
N3 / Radiation	23.9	10.875	0.0486	0.318	0.244
SQ2 / No radiation	2.38	4.55	-	0.336	-
SQ2 / Radiation	12.5	6.35	0.0323	0.407	0.161

References

- (1) B. O'Regan, M. Grätzel, *Nature* 1991, **353**, 737.
- (2) M. Law, L. E. Greene, J. C. Johnson, R. Saykally, P. Yang, *Nat. Mater.* 2005, **4**, 455-459.
- (3) A. Hagfeldt, G. Boschloo, L. Sun, L. Kloo, H. Pettersson, *Chem. Rev.* 2010, **110**, 6595-6663.
- (4) A. Sedghi, H. N. Miankushki, *Int. J. Electrochem. Sci.* 2012, **7**, 12078-12089.
- (5) C. Dwivedi, V. Dutta, A. K. Chandiran, MD. K. Nazeeruddin, M. Grätzel, *Energy Procedia* 2013, **33**, 223-227.
- (6) T.-T. Duong, J.-S. Choi, A.-T. Le, S.-G. Yoon, *J. Electrochem. Soc.* 2014, **161**, 166-171.
- (7) J. Wu, Z. Lan, J. Lin, M. Huang, Y. Huang, L. Fan, G. Luo, Y. Lin, Y. Xie, Y. Wei, *Chem. Soc. Rev.* 2017, **46**, 5975-6023.
- (8) H. Wang, P. Sun, J. Wu, L. Gao, Y. Wang, X. Dai, Q. Yi, G. Zou, *Nanoscale Res. Lett.* 2016, **11**, 27.
- (9) L. J. Bruce-Chwatt, *Bull World Health Organ.* 1956, **15**, 491-511.
- (10) F. Yuan, T. Yuan, L. Sui, Z. Wang, Z. Xi, Y. Li, X. Li, L. Fan, Z. Tan, A. Chen, M. Jin, S. Yang, *Nat. Commun.* 2018, **9**, 2249.
- (11) B. Viswanathan, S. Murugesan, A. riharan, K. S. Lakhi, *Adv. porous mater.* 2013, **1**, 122-128.
- (12) Y.H. Park, J.-S. Seo, S. Y. Park, J.-H. Lee, I. In, *Chem. Lett.* 2015, **44**, 685-687.
- (13) H. Wang, C. Sun, X. Chen, Y. Zhang, V. L. Colvin, Q. Rice, J. Seo, S. Feng, S. Wang, Y. W. William, *Nanoscale* 2017, **9**, 1909-1915.
- (14) T. N. Edison, A. Raji, M. G. Sethuraman, *J. Photochem. Photobiol. B-Biol.* 2016, **161**, 154-161.
- (15) J. F. Moulder, W. F. Stickle, P. E. Sobol, K. D. Bomben, Perkin-Elmer Corporation, Eden Prairie, 1992.

- (16) Z. R. Yue, W. Jiang, L. Wang, S. D. Gardner, C. U. Jr Pittman, *Carbon* 1999, **37**, 1785-1796.
- (17) Y. Xie, P. M. A. Sherwood, *Chem. Mater.* 1990, **2**, 293-299.
- (18) Z. Feng, Z. Li, X. Zhang, Y. Shi, N. Zhou, *Molecules* 2017, **22**, 2061.
- (19) D. Strle, B. Stefane, M. Trifkovic, M. V. Miden, I. Kvasic, E. Zupanic, I. Musevic, *Sensors* 2017, **17**, 2845.
- (20) D. Chen, W. Wu, Y. Yuan, Y. Zhou, Z. Wan, P. Huang, *J. Mater. Chem. C* 2016, **4**, 9027-9035.
- (21) C.-F. Lin, Y.-C. Chou, J.-F. Haung, P.-H. Chen, H.-C. Han, K.-Y. Chiu, Y. O. Su, *Jpn. J. Appl. Phys.* 2016, **55**, 03CE01.
- (22) Ministry of Government Legislation, Republic of Korea,
<http://www.law.go.kr/LSW/eng/engLsSc.do?menuId=2§ion=lawNm&query=nuclear+safety+act&x=0&y=0#liBgcolor15>, (accessed October 2019)
- (23) Ministry of Government Legislation, Republic of Korea,
<http://www.law.go.kr/LSW/eng/engLsSc.do?menuId=2§ion=lawNm&query=nclear+safety+act&x=0&y=0#liBgcolor7>, (accessed October 2019)
- (24) Korea Institute of Nuclear Safety, Republic of Korea,
<http://www.kins.re.kr/scale/service/law/view.do?lawSeq=71&historySeq=5&langTypeeng>, (accessed October 2019)
- (25) Nuclear Safety and Security Commission, Republic of Korea,
http://www.nssc.go.kr/nssc/en/nci/elif/Regulation_on_Technical_Standards_for_Raiation_Safety_Contro,ETC.pdf, (accessed October 2019)
- (26) F. Rahmani, H. Khosravinia, *Radiat. Phys. Chem.* 2016, **125**, 205-212.
- (27) A. Krasnov, S. Legotin, K. Kuzmina, N. Ershova, B. Rogozev, *Nucl. Eng. Technol.* 2019, **51**, 1978-1982.

- (28) M. V. S. Chandrashekar, C. I. Thomas, H. Li, M. G. Spencer, A. Lal, *Appl. Phys. Lett.* 2006, **88**, 033506.
- (29) A. Waris, Y. Kusumawati, A. S. Alfarobi, I. K. Aji, K. Basar, *AIP Conference Proceeding* 2016, **1719**, 030053.
- (30) Y. Ma, N. Wang, J. Chen, C. Chen, H. San, J. Chen, Z. Cheng, *ACS Appl. Mater. Interfaces* 2018, **10**, 22174-22181.
- (31) M. Lu, G.-G. Zhang, K. Fu, G.-H. Yu, D. Su, J.-F. Hu, *Energy Convers. Manag.* 2011, **52**, 1955-1958.